

# Epitaxial Volmer-Weber Growth Modelling

R. A. Coppeta\*, H. Ceric†, B. Karunamurthy‡, and T. Grasser\*

†Christian Doppler Laboratory for Reliability Issues in Microelectronics at the \*Institute for Microelectronics  
Technical University of Vienna, Gußhausstraße 27-29/E360, A-1040, Vienna, Austria

e-mail: {coppeta|ceric|grasser}@iue.tuwien.ac.at

‡KAI Kompetenzzentrum Automobil- u. Industrieelektronik GmbH

Europastraße 8, 9524 Villach, Austria

e-mail: bala.karunamurthy@k-ai.at

**Abstract**—As-deposited epitaxial thin III-nitride films grown on silicon substrates by vapor deposition often exhibit large intrinsic stress that can lead to film failure. The stress created in a III-nitride film is strictly related to its crystal structure evolution during its epitaxial Volmer-Weber growth on the Si substrate. Sensitive real-time measurements of stress evolution during the deposition show that the crystal structure evolution of the film can be divided into three main stages: an initial compressive stage caused by the nucleation of several islands of the film material on the substrate; a subsequent tensile stage associated with the coalescence of these islands ending at the percolation point with the formation of a continuous film; a final third compressive stage caused by the flux-driven incorporation of excess atoms within grain boundaries of the film. We propose a physically based analytical equation in order to obtain more insight into the stress-microstructure relation of the tensile stage of the growth, taking into account the epitaxial relation between the film and the substrate. The calculated values of the stress are compared with experimentally determined values of stress from the literature for an AlN thin film grown on a Si(111) substrate obtained through sensitive real-time measurements of the wafer bow. A comparison of the present model with experimental observations shows very good agreement using only a single fit parameter.

## I. INTRODUCTION

III-nitrides are considered promising semiconductors due to their wide band gap, high breakdown field, high electron mobility and sheet carrier density which make them ideal for power applications. Recently, III-nitride films have been grown on Si(111) substrate due to the low cost and wide availability of the silicon substrate. Unfortunately III-nitrides-on-Si-substrate based electronic chip production is yet to reach the required degree of reliability. Problems are partly due to the integration of III-nitrides thin films on Si substrates because they have different physical and chemical properties. In particular, the device performance is influenced by the stress in the films. We modelled the stress evolution during the Volmer-Weber epitaxial deposition of a thin film on the substrate. The theoretical results are compared with the experimental data from [1], that are referred to a AlN film grown on Si(111) substrate. AlN is commonly chosen as the first III-nitride layer to be grown on Si(111) because it has the lowest lattice mismatch with Si(111) in comparison with other III-nitride compounds.

## A. Stress evolution during the film growth

In principle, the stress in as-deposited epitaxial thin films arises when the film is subjected to any dynamical microstructural evolution process that changes the density of the film while it is rigidly attached to its substrate [2]. The stress increase can be understood in the following way: initially the film is stress-free and attached to the substrate; then, the film is ideally detached from the substrate; the growth induced physical phenomena happen, modifying the density of the film; then, the film is ideally reattached to the substrate and it is forced to have the same dimensions as the substrate. Now the film is in a state of stress that is imposed by the dimensional constraint of the thicker substrate. The film imposes forces and moments on the substrate and consequently the substrate bends slightly. The substrate curvature can be measured and related to stress into the film by the Stoney formula [3]. Since we are dealing with Si(111), we use [4]:

$$\sigma_f t_f = \left( \frac{6}{4s_{11} + 8s_{12} + s_{44}} \right) \frac{h_f^2}{6r}, \quad (1)$$

where  $\sigma_f$  is the stress in the film,  $t_f$  is the growth time,  $s_{11}$ ,  $s_{12}$ ,  $s_{44}$  are the compliance terms of Si(100) tensor,  $h_f$  is the film thickness,  $r$  is the curvature radius of the substrate. Using the experimental data of the curvature reported in [1], it is possible to calculate the stress in the film as a function of the growth time  $t$ . A typical stress development as a function of thickness that can be related to the growth time through the growth rate is shown in Fig.1. The main observation in Fig. 1 is that the stress evolves from compressive to tensile and then back to compressive, which is referred to as CTC behavior [5]. The main difference between Fig.1 and the experimental data obtained from [1] is the lack of the first compressive stage in [1]. This lack is caused probably by the low impact of this stage in the AlN grown on Si(111) and by the low sensitivity of the instruments used. The tensile and compressive stages have been directly related with the microstructural evolution [6]. The rapid tensile rise is related to the onset of island coalescence and grain-boundary formation. The peak in the tensile curvature occurs when the film becomes fully continuous. The final compressive stage observed in the continuous film is caused by the incorporation of high-mobility ad-atoms into the grain boundaries previously created.

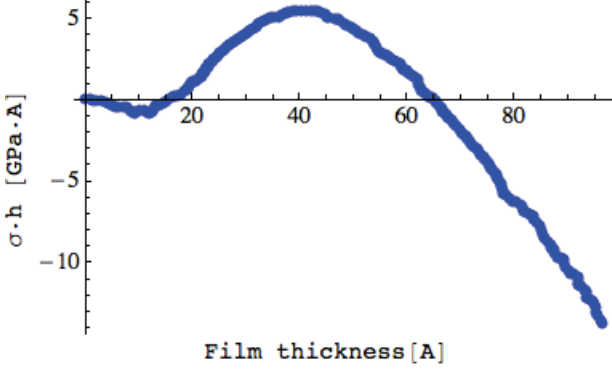


Fig. 1. Real time substrate-curvature measurements during ultrahigh-vacuum evaporation of amorphous Ge. Positive values of stress-thickness correspond to mean tensile stress, while negative values correspond to compressive stress [6].

### B. Island coalescence regime

The rapid increase in tensile stress is related to the onset of island coalescence to form grain boundaries and to the lattice mismatch between the film and the substrate. Since there are only empirical models of the coalescence process before the percolation point [7], we propose a physically based analytical equation (2) in order to obtain more insight into the stress-microstructure relation of this stage. The model takes into account the stress arising from the grain boundary formation and the stress arising from the lattice mismatch between the AlN layer and Si(111). Several assumptions are made: islands are supposed to have the same grain size, to be hemispherical, isotropic, and to coalesce at the same moment. Based on these hypotheses we suggest an equation describing the stress behaviour during the coalescence process:

$$\sigma(t) = \sigma_{xx}(t) = \sigma_{yy}(t) = c + \frac{M_f \epsilon_m b_x v_{gr} t}{R^2} + \frac{\gamma v_{gr}^2 t^2}{2R^3}, \quad (2)$$

where  $c$  is a constant that quantifies the stress caused by island nucleation and is the only fitting parameter.

The second term quantifies the stress caused by the lattice mismatch between AlN and Si. The stress field caused by the misfit of the lattice parameters of the thin film and the substrate is generally a biaxial stress with the only non-zero components

$$\sigma_{xx} = \sigma_{yy} = \sigma_m, \quad (3)$$

where  $\sigma_m$  is the misfit stress. This is true for isotropic materials as well as for wurtzite materials where the interface is the c-plane (in which all directions are equivalent). The matrix of the misfit stress is

$$\sigma_m = \begin{pmatrix} \sigma_m & 0 & 0 \\ 0 & \sigma_m & 0 \\ 0 & 0 & 0 \end{pmatrix}.$$

The total misfit force acting on the dislocation whose Burgers vector x-component is  $b_x$  is [8]

$$F_m = \sigma_m b_x h_f = \epsilon_m M_f b_x h_f = \epsilon_m M_f b_x v_{gr} t. \quad (4)$$

This force increases with the film thickness  $h_f = v_{gr} t$ .  $M_f$  is the biaxial modulus of the AlN film,  $\epsilon_m$  is the lattice mismatch strain between Si(111) and AlN,  $b_x$  is the x-component of the Burger vector,  $v_{gr}$  is the film growth rate, and  $t$  is the growth time. The misfit strain in the epilayer is taken as

$$\epsilon_m = \left( \frac{a_s - a_f}{a_f} \right). \quad (5)$$

This definition of the misfit strain is based on the idea that the thin film in-plane lattice constant adjusts to the rigid substrate lattice constant [9]. The lattice parameters can be found considering the epitaxial relationship between the substrate and the film [10]. The (111) plane is the most commonly used surface of Si for growth of the group III-nitrides [11]. The epitaxial orientation relationship in general is  $\{111\}_{Si} \langle \bar{1}00 \rangle_{Si} // \{0001\}_{AlN} \langle 11\bar{2}0 \rangle_{AlN}$ . The sixfold symmetry of arrangement of atoms on the unreconstructed  $\{111\}$  surface favors the growth of the wurtzite phase with hexagonal symmetry. The mismatch defined in (5) is greater than 20% for AlN and of a nature that would result in a tensile (or positive) stress in the film when grown directly on Si(111). It should be noted that for Si(111),  $a_s$ , given the orientation relationship, should be the interatomic distance along  $[1\bar{1}0]$  and not the often quoted lattice parameter of Si, which is the interatomic distance along  $[110]$ .  $R$  is the average grain size. In order to calculate the stress,  $F_m$  has to be divided by the contact area between two hemispherical grains. The contact area is  $\pi R^2$ , approximated to  $R^2$ . In order to get an estimation of the average grain size  $R$  of the AlN film, the maximum stress at the percolation point is considered. The Nix-Clemens [12] and Freund-Chason [13] models are often applied to predict the maximum stress at the percolation point during the growth. Nix and Clemens [12] imagined the grain boundary formation as a crack-closure process. The surfaces of adjacent grains are considered like the crack surfaces. At the point of contact, the crack closes attaching the two surfaces, reducing the total surface energy while creating elastic strain. This process is equivalent of the Griffith's criterion for crack propagation. According to their model, the resulting stress is

$$\sigma = \sqrt{\frac{M_f \gamma}{R}}. \quad (6)$$

In order to consider more realistic island geometries, Freund and Chason [13] developed a new model based on the contact theory of elastic solids with cohesive attraction between them. According to their model, the maximum stress among 3D islands is

$$\sigma = \frac{4\gamma}{R}. \quad (7)$$

Since it is possible to get the value of the maximum stress from Fig. 2, we apply these models to get the related average grain size. The Nix-Clemens result overestimates the experimental maximum stress by two orders of magnitude. The Freund-Chason one is close to the experimental value (Fig. 3). Based on this comparison, we use the Freund-Chason model to obtain an estimate of the average grain size of the film.

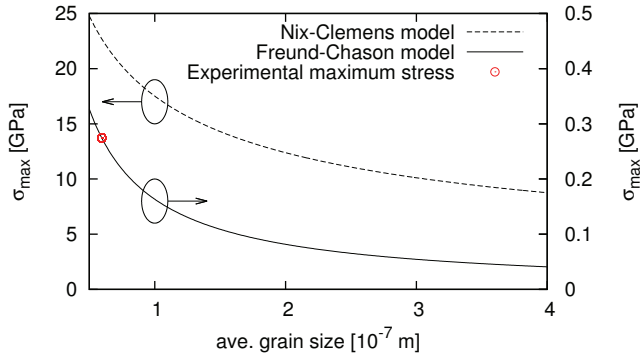


Fig. 2. Comparison between the Nix-Clemens and Freund-Chason models. The Nix-Clemens model dramatically overestimates our experimental maximum stress value.

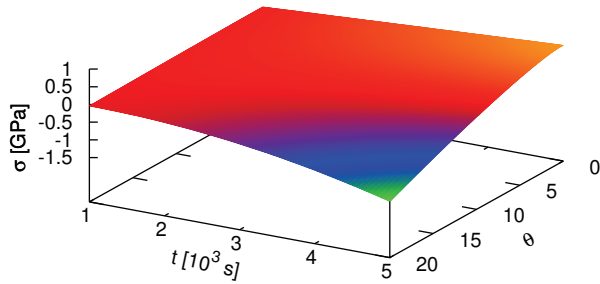


Fig. 3. Stress as a function of  $\theta$  and time.

The third term quantifies the grain boundary formation effect on the stress. Hoffman [14] suggested that a tensile stress could be generated in the film as the islands make contact with their neighboring islands. The reason behind this suggestion is that the net surface energy of the islands could be lowered by some amount if they joined in forming a grain boundary whose surface energy is less than the energy associated with the solid-vapour interface of the islands. The deformation of an island as a result of the adjacent grain boundary formation results in an increase in its elastic strain energy. The process of forming these shared boundaries can proceed spontaneously since this process is associated to a decrease of the total energy of the structure.  $\gamma$  is the difference between the  $\gamma_s$ , which is the solid-vapour interface energy, and  $\gamma_{gb}$ , which is the grain boundary energy. The solid-vapour interface energy  $\gamma_s$  can be estimated through [15]:

$$\gamma_s \approx \frac{E_{coh} N Z_b}{Z}, \quad (8)$$

where  $E_{coh}$  is the cohesive energy of the chemical bond,  $Z$  is the number of bonds formed by one atom in the bulk,  $Z_b$  is the number of dangling bonds of one atom along the surface,  $N$  is the number of atoms per unit surface.

The grain boundary energy  $\gamma_{gb}$  can be estimated considering

that several experimental observations [1] [11] confirm the formation of low angle boundaries. AlN, like all III-nitride films, on silicon substrates has domains that are twisted or tilted with respect to the substrate-film interface to varying extents. The difference in twist and in tilt between domains can be accommodated by low angle grain boundaries. Low angle grain boundaries are interfaces between domains with a misorientation angle  $\theta$  less than about  $11^\circ$ . They are composed of an array of dislocations and their properties and structure are a function of the misorientation [16]. The difference in twist can be accommodated by low angle grain boundaries composed by pure edge dislocations, whereas a difference in tilt can be accommodated by low angle grain boundaries composed by pure screw dislocations. When a combination of both difference in twist and tilt between domains exists, then all three types of dislocations create low angle grain boundaries. The dislocations observed composing the low angle grain boundaries in AlN films are of three types,  $a$ ,  $c$ , and  $a+c$ . The  $a$ -type dislocations are pure edge dislocations, with Burgers vector  $\mathbf{a}$  ( $1/3 \langle 11\bar{2}0 \rangle$ ) and a dislocation line along the  $c$ -axis. The  $c$ -type dislocations are pure screw dislocations with a Burgers vector  $\mathbf{c}$  ( $\langle 0001 \rangle$ ) and a line direction along the  $c$ -axis. The  $a+c$  type dislocations are mixed dislocations with Burgers vector  $\mathbf{a} + \mathbf{c}$  ( $1/3 \langle 11\bar{2}3 \rangle$ ) with line direction inclined at  $12.2^\circ$  to the  $c$ -axis [17]. It is pointed out that a pure twist between domains with respect to the substrate results in pure tilt grain boundaries between them in the film. Pure tilt with respect to the substrate could result in tilt boundaries, twist boundaries, or a combination. While reported fractions vary greatly, the  $a$ -type constitutes about 70%–90% of the population, the remainder being made up of the  $c$  and  $a+c$  type [18]. As a consequence we modelled only low angle grain boundaries composed by  $a$ -type dislocations. The energy  $\gamma_{gb}$  of these grain boundaries can be estimated as a function of the misorientation angle  $\theta$  and the Burgers vector  $\mathbf{b}$  according to the theory of dislocations [16]. The parameters regarding this kind of dislocations in III-nitrides can be found in [9]. Based on the theory of dislocations [16], the grain boundary energy can be calculated as

$$\gamma_{gb} = \frac{\mu_f b \theta}{4\pi(1-\nu_f)} \ln\left(\frac{eb}{2\pi\theta r_0}\right), \quad (9)$$

where  $\theta$  is the misorientation angle between grains which is less than  $11^\circ$  for low angle grain boundaries. It is found that  $\theta$  has a small influence on the final stress (Fig. 4).  $\mu_f$  and  $\nu_f$  are the shear modulus and Poisson ratio of AlN,  $b$  is the Burgers vector modulus and  $r_0$  is the core radius of the single dislocation. All parameter values used in (2)(5)(7)(8)(9) are in Table I.

### C. Atom insertion in grain boundaries

The post-coalescence stage is characterized by the insertion of ad-atoms in grain boundaries. In equilibrium, the grain boundary and the surface have the same chemical potential so there is no net flux between them. During deposition, however, condensation of atoms from the vapor increases the surface

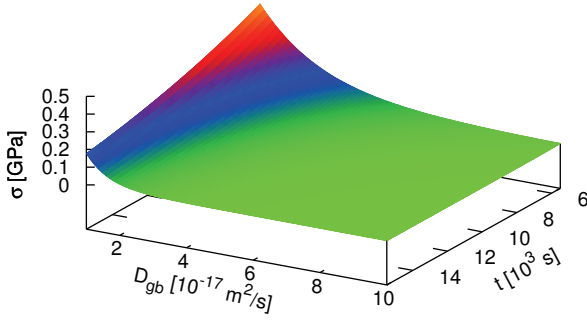


Fig. 4. Stress as a function of  $D_{gb}$  and time.

chemical potential through the excess ad-atom population. The excess chemical potential of the growth surface relative to the grain boundary produces a net flux of atoms into the boundary that generates a compressive stress in the film. The flow of atoms will continue until the resultant compressive stress forces the chemical potential of the grain boundary to equal the chemical potential of the growth surface, and a steady state is achieved. This process in a thin film is modeled according to [19] :

$$\sigma(t) = \sigma_{xx}(t) = \sigma_{yy}(t) = \pi \sigma_{\max} e^{-\frac{t}{t_0}} \quad (10)$$

$$\text{with } t_0 = \frac{4\pi (1 - \nu_f^2) v_{gr} k_B T t_{\max}^3 \sigma_{\max}}{Y_f b_x D_{gb} \Omega}, \quad (11)$$

where  $\sigma_{\max}$  is the maximum stress reached during the growth,  $\nu_f$  is the film Poisson ratio,  $k_B$  is the Boltzmann constant,  $T$  is the deposition temperature,  $t_{\max}$  is the maximum stress time,  $Y_f$  is the AlN film Young modulus,  $D_{gb}$  is the diffusion coefficient along grain boundaries fitted to experimental data,  $\Omega$  is the atomic volume calculated through the mixing rule with Al and N atomic volumes. All parameter values used in (10) and (11) are summarized in Table I. The variation of  $D_{gb}$  has an impact on the stress that cannot be neglected for small values (Fig. 5). The impact of the lattice mismatch between AlN islands and Si substrate on the stress development during Volmer-Weber growth is demonstrated in Fig. 6, where we find a good agreement between our theoretical results and the experimental data.

## II. CONCLUSION

We have suggested a model that captures the relation between the microstructure evolution and the stress development during the Volmer Weber growth, in particular showing the impact of both the film-substrate lattice mismatch and the grain boundary formation during the coalescence process of the islands. Excellent agreement with experimental data is obtained using only a single fit parameter. The equations can be improved in order to better model the transition zone between the tensile and the compressive stages, where the grain boundary formation and the atom insertion overlap each

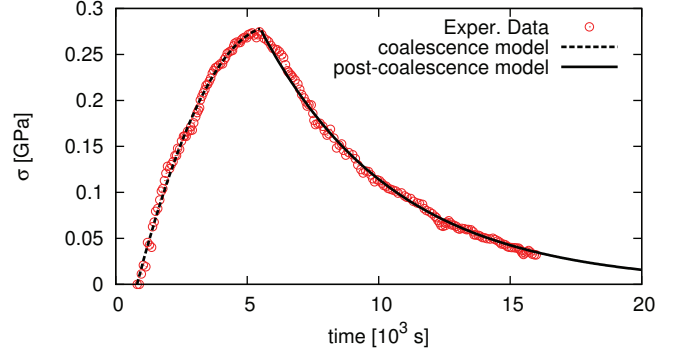


Fig. 5. Comparison between the experimental data and the model results.

other. Other improvements can be derived relaxing several of the ideal conditions imposed here. These assumptions are that the islands are hemispherical, have the same size and coalescence in the same moment. The diffusion coefficient along the grain boundaries should be found experimentally. Whole the model is based on the assumption that the AlN film is polycrystalline. Recent observations [20] propose an alternative view of the microstructure, but more studies are necessary to close the diatribe.

TABLE I

THE PARAMETERS USED ARE TAKEN FROM LITERATURE, EXCEPT FOR  $N$ ,  $Z_b$ ,  $Z$ , WHICH ARE CALCULATED, AND  $c$ , WHICH IS FITTED.

$Y_f$	$\nu_f$	$\epsilon_m$	$b$	$b_x$	$r_0$	$E_{coh}$
308 GPa	0.18	0.235	0.5871 nm	0.58 nm	b/2	2.88 eV
[10]	[10]	[11]	[9]	[9]	[9]	[10]
$N$	$Z_b$	$Z$	$\Omega$	$v_{gr}$	$T$	$c$
12.9 fm <sup>2</sup>	1	4	13.65 cm <sup>3</sup> /mol	90 nm/h	750°C	-0.095 GPa
calc.	calc.	calc.	calc.	[1]	[1]	fit.

## REFERENCES

- [1] B. Sheldon *et al.*, Journal of Applied Physics **98**, 043509 (2005).
- [2] M. Doerner *et al.*, CRC Crit. Rev. Solid State Mater. Sci. 225 (1988).
- [3] G. Stoney, Thin Solid Films **A 82**, 172 (1909).
- [4] G. Janssen *et al.*, Thin Solid Film **517**, 1858 (2009).
- [5] J. Floro *et al.*, MRS BULLETIN 19 (2002).
- [6] J. Floro *et al.*, Journal of Applied Physics **89**, 4886 (2001).
- [7] S. Seel, Ph.D. thesis, Massachusetts Institute of Technology, 2002.
- [8] L. Freund *et al.*, *Thin Film Materials* (Cambridge University Press, 2003).
- [9] D. Holec, Ph.D. thesis, University of Cambridge/Selwyn College, 2006.
- [10] H. Morkoc, *Handbook of Nitride Semiconductors and Devices* (WILEY VCH Verlag, 2008).
- [11] T. Li *et al.*, *III-V Compound Semiconductor* (CRC Press, 2011).
- [12] W. Nix *et al.*, Journal of Materials Research **14**, 3467 (1999).
- [13] L. Freund *et al.*, Journal of Applied Physics **89**, 4866 (2001).
- [14] R. Hoffman, Journal of Applied Physics **34**, 185 (1976).
- [15] J. Venables, *Introduction to Surface and Thin Film Processes* (Cambridge University Press, 2003).
- [16] J. Hirth *et al.*, *Theory of dislocations* (Krieger Publishing Company, 1982).
- [17] S. Mathis *et al.*, J. Cryst. Growth 231 (2001).
- [18] D. Follstaedt *et al.*, MRS Internet J. Nitride Semicond. Res. (1999).
- [19] H. Gao *et al.*, Acta Materialia **47**, 2865 (1999).
- [20] M. Moram *et al.*, Journal of Applied Physics **106**, 073513 (2009).